Supplementary Information

Multifunctional polyurethane hydrogel based on phenol-carbamate network and Fe^{3+}-polyphenol coordination bond toward NIR light triggered actuators and strain sensors

Yang Liu [a, b], Zetian Zhang [a, b], Ze Liang [a, b], Yong Yong [a, b], Changkai Yang [a, b], Zhengjun Li [a, b, *]

[a]*National Engineering Research Center of Clean Technology in Leather Industry, Sichuan University, Chengdu, 610065, China*

[b]*Key Laboratory of Leather Chemistry and Engineering of Ministry of Education, Sichuan University, Chengdu, 610065, China*

* Corresponding author: lizhengjun@scu.edu.cn (Z. J. Li)

Materials and methods

Materials

Isophorone diisocyanate (IPDI) was purchased from Chengdu Huaxia Chemical Reagent Co., Ltd. Polyethylene glycol (PEG, Mn = 4000), poly(propylene glycol) (PPG, Mn = 1000), 1, 4-butanediol (BDO), N, N-dimethylformamide (DMF), dibutyltin dilaurate (DBTDL), $FeCl_3 \cdot 6H_2O$, $CuSO_4 \cdot 5H_2O$, ethylenediaminetetraacetic acid (EDTA), and 4 Å molecular sieves were obtained from Chengdu Kelong Chemical Reagent Co., Ltd. Tannic acid (TA, 98%, Mw = 1701.2) was supplied by Shanghai Aladdin Biochemical Technology Co., Ltd. Trimethylolpropane (TMP) was provided by Shanghai Titan Scientific Co., Ltd. PEG and PPG were dehydrated under reduced pressure at 120 °C for 2 h before use. BDO and DMF were dried by using 4 Å molecular sieves before use. All of the reagents above except IPDI were analytical grade.

Preparation of tannic acid-based polyurethane (TAPU) solution

TAPU polymers were prepared by a stepwise polymerization method, and the compositions are shown in Table S1. A typical procedure is described as follows (using TAPU-3 as an example): firstly, IPDI (4.44 g, 20.00 mmol), PEG (10.00 g, 2.50 mmol), PPG (5.00 g, 5 mmol), and two drops of DBTDL were added into a four-neck flask (250 ml) and stirred at 85 °C for 2 h under N_2 atmosphere. Subsequently, BDO (0.29 g,

3.22 mmol) was dropped into the above oligomer, after reacting for 1 h, the linear and NCO-terminated polyurethane prepolymer was obtained. After that, a defined amount of TA (3.00 g, 1.76 mmol) dissolved in DMF was fed into the above mixture. Finally, tannic acid-based polyurethane solution with phenol-carbamate network was obtained after stirring at 85 °C for extra 4 h.

For comparison, chemically cross-linked TMPU without phenol-carbamate network was fabricated according to the preparation procedure of TAPU-3 by substituting TMP for TA.

Table S1. Compositions for synthesizing TAPU polymers.

Samples	IPDI (mmol)	PEG (mmol)	PPG (mmol)	BDO (mmol)	TA (mmol)
TAPU-1	20.00	2.50	5.00	6.11	1.17
TAPU-2	20.00	2.50	5.00	4.67	1.47
TAPU-3	20.00	2.50	5.00	3.22	1.76

Preparation of NIR-responsive and conductive TAPU/Fe hydrogel

The TAPU/Fe hydrogel was prepared according to the following steps. Briefly, TAPU hydrogel was firstly fabricated, that is, the above TAPU solution was poured into PTFE mold (80 mm × 80 mm × 10 mm), cured at ambient temperature overnight, and then dried in convection oven at 60 °C for 48 h. After peeling from the mold, the cured TAPU film was immersed in deionized water at ambient temperature for different time (from 0 to 180 min) to yield the TAPU hydrogel. Subsequently, the TAPU/Fe hydrogels were obtained by immersing the cured TAPU-3 film in different concentrations of $FeCl_3$ aqueous solution (100 mL) at ambient temperature for 2 h. The molar ratio of TA to Fe^{3+} is 1 to 3.70, 18.4, 36.8, 55.2, and 73.6, for easy naming, the corresponding hydrogels were denoted as TAPU/Fe-1, TAPU/Fe-2, TAPU/Fe-3, TAPU/Fe-4, and TAPU/Fe-5, respectively.

Characterization

Fourier transform infrared (FT-IR) spectra were collected on a Spectrum 3 instrument (PerkinElmer, USA). ^{1}H NMR spectrum was carried out on an AV II-600 MHz (Bruker, Switzerland) spectrometer using DMSO-d_6 as a deuterated solvent. UV-

vis spectra were recorded using a UV spectrophotometer UV-3900H (Hitachi, Japan) in the range of 250 to 900 nm under room temperature, the concentration of each TAPU solution was 8.5×10^{-5} g/mL, and the concentration of each TAPU/Fe solution was 6.25×10^{-3} g/mL. Differential scanning calorimetry (DSC) was carried out on a DSC 204 F1 (Netzsch, Germany). The cured TAPU films were heated from 0 to 80 °C at a rate of 10 °C/min under nitrogen atmosphere. The volume phase transition temperature (VPTT) of hydrogels was also determined by DSC, each sample was sealed in a hermetic pan and heated from 30 to 60 °C at a rate of 5 °C/min under nitrogen atmosphere. X-ray diffraction (XRD) analysis was performed on an X′ Pert Pro MPD DY129 diffractometer (Panalytical, Holland) from 2θ angle of 4° to 60° using CuKα radiation (λ=1.541 Å) at a scanning speed of 4°/min. Swelling behavior of the TAPU hydrogels was determined by a gravimetric process. Each dry gel film was immersed in deionized water at room temperature, and the samples were weighed at stipulated time points after removing any excess water on the surface. Five measurements were carried out for each sample, and the swelling ratio of the hydrogels was calculated by using the equation (1).

$$\text{Swelling ratio (\%)} = (W_s\text{-}W_d)/W_d \times 100\% \quad (1)$$

where W_s and W_d are the mass of swollen and dried hydrogels, respectively.

Deswelling ratio (%) of the hydrogels was defined as the equation (2).

$$\text{Deswelling ratio (\%)} = (W_0\text{-}W_t)/W_0 \times 100\% \quad (2)$$

where W_0 is the mass of the equilibrium swollen hydrogel at 25 °C, and W_t is the mass of the hydrogels during the dehydration process at different temperatures.

Scanning electron microscopy (SEM) image of the hydrogels was observed under the field emission scanning electron microscopy (FE-SEM) (Apreo S HiVac FEI, Thermo Scientific, USA) equipped with an EDS detector. The cross-section morphology and element distribution of the hydrogels were directly recorded by SEM-EDS. The swollen hydrogels were frozen in liquid nitrogen, freeze-dried for 48 h, and then coated with gold before observation. Mechanical tests of the hydrogels with a dumb-bell shape (~50 mm × 4 mm × 0.8 mm) were performed using a UTM 6203 universal material testing machine (Suns, China) according to ASTM D-638 standard

at a stretch speed of 100 mm/min under room temperature. The cyclic tensile tests were carried out for 10 loading-unloading cycles at 100 mm/min and strain of 100% without intervals between consecutive cycles. Elemental analysis for the dried hydrogels was based on X-ray photoelectron spectroscopy (XPS) (AXIS Ultra DLD, UK).

Photothermal effect of the hydrogels. The hydrogel films (~30 mm × 6 mm × 0.8 mm) were exposed upon NIR laser (800-1100 nm, 1.0 W/cm^2) with a distance of ~12 cm, and the real-time temperature was collected by E5 infrared thermographic camera (FLIR, USA). The reversible photothermal effect of the hydrogels was estimated by repeated irradiation. The hydrogels were firstly irradiated by NIR light for 2 min, and then the laser was turned off to allow the temperature to decrease to room temperature. Subsequently, the hydrogels can again reach swelling equilibrium in water. The whole process was repeated three times, and the real-time temperature was recorded.

NIR induced deswelling ratio of the hydrogels. Briefly, the water on the surface of the swollen hydrogels was wiped off by filter paper, and then the swollen hydrogels were weighted as W_1. Subsequently, the swollen hydrogels were irradiated by NIR light for different times, and the water on the surface of the hydrogels was wiped off, then the hydrogels were weighted (W_t) at stipulated time points. The NIR triggered deswelling ratio of the swollen hydrogels was calculated by using the equation (3).

$$\text{NIR triggered deswelling ratio (\%)} = (W_1\text{-}W_t)/W_1 \times 100\% \quad (3)$$

NIR triggered actuation of the hydrogels. Firstly, one end of the rectangular hydrogels (~30 mm × 6 mm × 0.8 mm) was fixed, and then the samples were irradiated by NIR light with a distance of ~12 cm for 2 min. The NIR triggered bending behavior of the hydrogels can be seen intuitively, and the bending angle was measured at the corresponding time point. When the NIR light was turned off, the bending hydrogels can return to its original shape by immersing in water. The whole procedure was repeated three times, and the bending angle was also recorded.

The electrical signals of the hydrogels were collected by an electrochemical workstation (CHI760E, China). The conductivity (δ, mS/cm) of the hydrogels was calculated according to the following equation (4).

$$\delta = L/(R \times S) \quad (4)$$

where L is the length between two adjacent probes (cm), R is the resistance of the hydrogel (Ω), and S represents the cross-sectional area of the hydrogel (cm^2). The real time resistance changes of the hydrogels were recorded by the electrochemical workstation at 1 V voltage. The strain sensitivity of the tensile testing was defined as the following equation (5).

$$GF = ((R-R_0)/R_0)/\varepsilon \quad (5)$$

where R_0 and R are the instantaneous resistance values without and with applied strain, ε is the strain of the hydrogel. The practical applications of the hydrogel sensor were conducted at room temperature. The prepared hydrogel sensor was fixed on the volunteer's forefinger, wrist, and throat to monitor the human motions, and the real time electrical signals caused by various motions were collected by electrochemical workstation at 1 V voltage. Similarly, the prepared hydrogel was used to discern handwritings by writing directly on the surface of the assembly hydrogel sensor, the 2D distribution of force and strain can be detected.

Temperature-variable FT-IR spectra were collected on a Spectrum 3 instrument (PerkinElmer, USA) equipped with a hot stage. The dried hydrogel (TAPU/Fe-4) was firstly dissolved by DMF and cast on a KBr window plate to obtain a thin film, and then transferred into the hot stage. Subsequently, the transmission spectra were collected at a resolution of 4 cm^{-1} in the region of 4000 to 600 cm^{-1} after the sample was equilibrated at programed temperature for 3 min.

Recycling test. The dried hydrogel (TAPU/Fe-4) was dissolved in DMF at 120 °C for 2 h, and then the solution was poured into the PTFE mold. After curing at 85 °C for 24 h, the phenol-carbamate network can be reconnected. Subsequently, the cured film was immersed in deionized water again to obtain the recycled hydrogel.

The cell viability was determined using Cell Counting Kit-8 (CCK-8) assay. Firstly, the prepared hydrogel was cut into 10 mm × 10 mm rectangles and sealed before ^{60}Co irradiation sterilization. Subsequently, the sterilized hydrogels were placed into a 96-well plate and L929 fibroblasts were co-cultured with the extract at 37 °C with 5% CO_2 in the air for 1, 3, and 5 days. CCK-8 was utilized to determine the number of active cells indirectly. Besides, L929 fibroblasts were inoculated directly onto the

prepared samples and co-cultured at 37 °C with 5% CO_2 in the air for 1, 2, and 3 days. For cell observation and photography, confocal laser scanning microscopy (CLSM) (Leica, Germany) was applied after the TRITC-phalloidin staining.

Fluorescence spectra (excitation and emission) of the TAPU hydrogels were collected at room temperature using a F-7000 fluorescence spectrometer (Hitachi, Japan). The fluorescence quenching effect of Cu^{2+} was evaluated by adding Cu^{2+} solution (50 μL) with different concentrations (0-100 mM) into TAPU solution (0.015 g/mL, 4 mL). After completely mixing, the emission spectra (E_x=360 nm) of the corresponding mixture were recorded. Filter papers containing Cu^{2+} were prepared by immersing blank filter papers into $CuSO_4$ solution (10 mM) for 2 h, and then dried in an oven (60 °C). Subsequently, the dried filter papers containing Cu^{2+} were tailored into various shapes. For ionoprinting, various tailored filter papers containing Cu^{2+} were covered on the surface of TAPU hydrogels at room temperature for different times. For erasing, the quenched TAPU hydrogels were soaked in EDTA solution (20 mM) for 5 min, and the photos of the TAPU hydrogels after being treated by Cu^{2+} or EDTA were collected under UV light (365 nm).

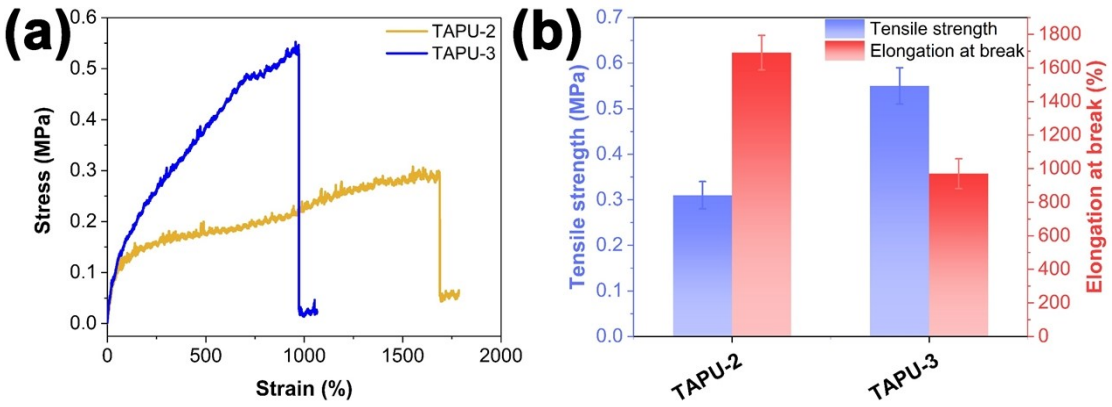

Fig. S1. (a) Representative stress-strain curves and (b) mechanical data of TAPU-2 and TAPU-3 hydrogels.

Fig. S2. Appearance of TAPU-3 and TAPU/Fe hydrogels.

Table S2. Chemical compositions of TAPU-3 and TAPU/Fe-4 hydrogels as determined by XPS.

Sample	Composition (at %)			
	C	O	N	Fe
TAPU-3	73.38	24.36	2.26	--
TAPU/Fe-4	72.68	23.62	3.42	0.28

Table S3. Mechanical properties of some previously reported hydrogels.

Hydrogel samples	Tensile strength (MPa)	Elongation at break (%)	References
PU hydrogel	0.37	37	Mater. Sci. Eng. C 2021, 131, 112520.
PAM/TA@CNFs hydrogel	0.11	135	Carbohydr. Polym. 2020, 250, 117010.
Poly(AA-co-SMA)/c-CNF/Fe^{3+} hydrogel	0.09	902	Colloids Surf. A 2020, 592 124587.
PDA/CMC-Fe^{3+}/PVA hydrogel	0.16	233	Compos. Sci. Technol. 2021, 206, 108653.
PVA/Chitosan/Cyclodextrin hydrogel	0.50	314	Ind. Eng. Chem. Res. 2022, 61, 3620-3635.
PAM-CNF nanocomposite hydrogel	0.29	691	ACS Appl. Mater. Interfaces 2022, 14 10886-10897.
TAPU/Fe-4 hydrogel	0.75	550	This work

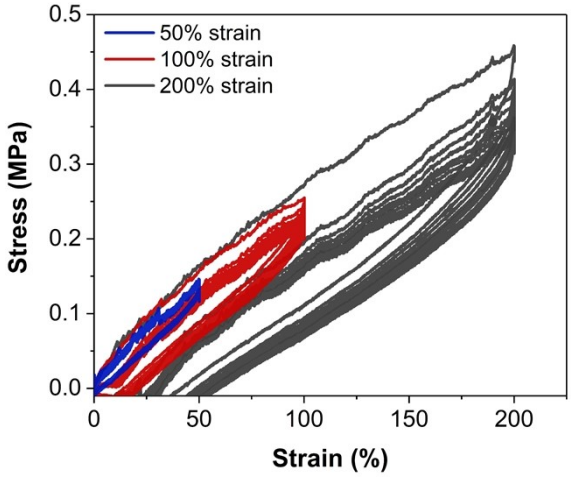

Fig. S3. Ten successive loading-unloading cycles at 50%, 100%, and 200% strains of TAPU/Fe-4 hydrogel.

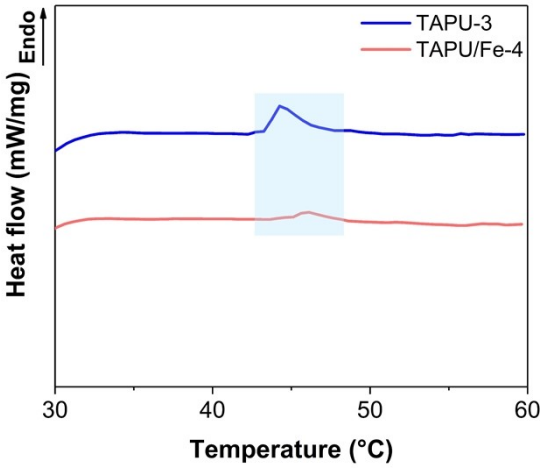

Fig. S4. DSC curves of TAPU-3 and TAPU/Fe-4 hydrogels.

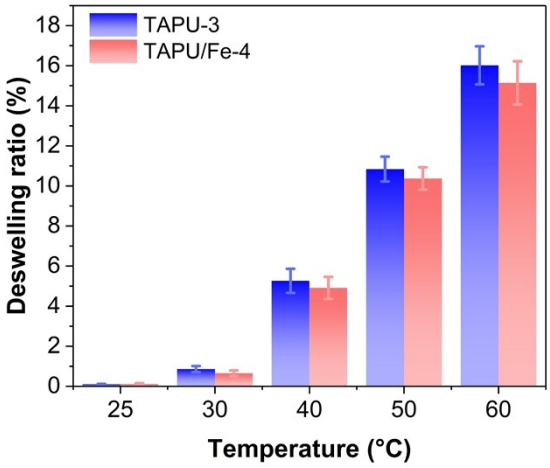

Fig. S5. Deswelling behaviors of the swollen TAPU-3 and TAPU/Fe-4 hydrogels at different temperatures.

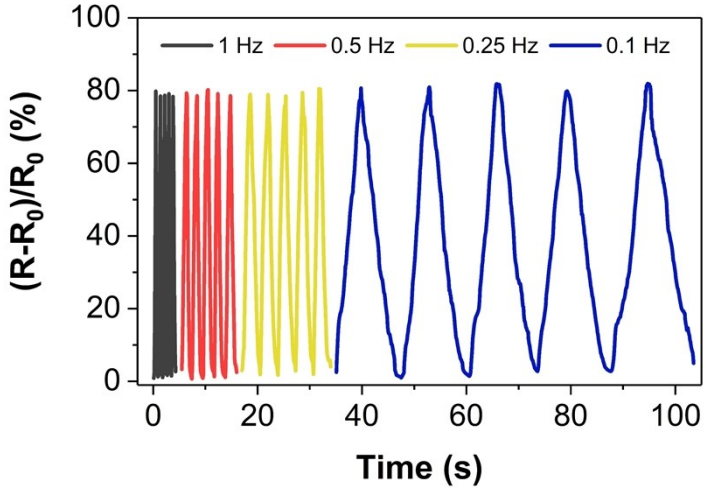

Fig. S6. Relative resistance changes of TAPU/Fe-4 hydrogel in response to different stretching frequencies.

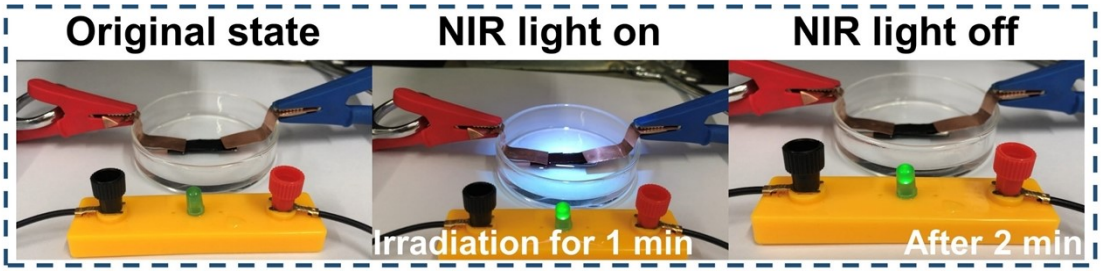

Fig. S7. The brightness of the LED bulb dimmed after turning off the NIR light for 2 min.

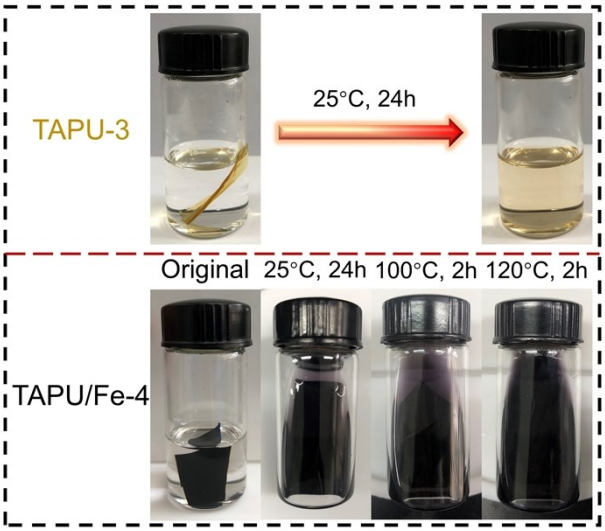

Fig. S8. Swelling behaviors of the dry TAPU-3 and TAPU/Fe-4 films after being soaked in DMF at different temperatures.

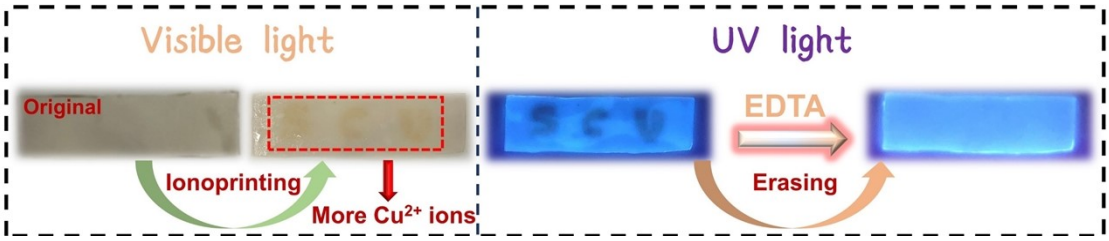

Fig. S9. Photos of the hydrogel pattern treated with Cu^{2+} ions (extending the contacting time between the hydrogel and filter papers to 5 min) and EDTA.